

AperTO - Archivio Istituzionale Open Access dell'Università di Torino

## Surface Interactions of Arsenite and Arsenate on Soil Colloids

### **This is the author's manuscript**

*Original Citation:*

*Availability:*

This version is available <http://hdl.handle.net/2318/146525> since 2018-03-30T16:20:47Z

*Published version:*

DOI:10.2136/sssaj2013.04.0133

*Terms of use:*

Open Access

Anyone can freely access the full text of works made available as "Open Access". Works made available under a Creative Commons license can be used according to the terms and conditions of said license. Use of all other works requires consent of the right holder (author or publisher) if not exempted from copyright protection by the applicable law.

(Article begins on next page)



# UNIVERSITÀ DEGLI STUDI DI TORINO

*This is an author version of the contribution published on:*

*Questa è la versione dell'autore dell'opera:*

*Soil Science Society of America Journal, 78 (1), 157-170. 2014.*

*DOI:10.2136/sssaj2013.04.0133*

*The definitive version is available at:*

*La versione definitiva è disponibile alla URL:*

<https://www.soils.org/publications/sssaj/articles/78/1/157>

## TITLE PAGE

### **Surface interactions of arsenite and arsenate on soil colloids**

Maria Martin<sup>1\*</sup>, A. Violante<sup>2</sup>, F. Ajmone-Marsan<sup>1</sup>, E. Barberis<sup>1</sup>

<sup>1</sup> Università di Torino, DISAFA – Chimica Agraria e Pedologia, Via L. da Vinci 44, 10095 Grugliasco (Torino), Italy.

<sup>2</sup> Università di Napoli Federico II, Dipartimento di Agraria, Via Università 100, 80055 Portici, (Napoli) – Italy.

## CORRESPONDING AUTHOR

Maria Martin<sup>\*</sup>, Università di Torino, DISAFA – Chimica Agraria e Pedologia, Via L. da Vinci 44, 10095 Grugliasco (Torino), Italy.

Telephone: +39-011 6708512; Fax: +39-011 6708692

Email address: [maria.martin@unito.it](mailto:maria.martin@unito.it)

## **ABBREVIATIONS**

KGa2: Kaolinite from Georgia (Clay Mineral Society); KGa2-Fh: Kaolinite with co-precipitated Ferrihydrite; XRD: X-ray diffractometry; LDV-PCS: Laser Doppler Velocimetry – Photon Correlation Spectroscopy; ITC: Isothermal Titration Calorimetry; SSA: Specific Surface Area; PZC: Point of Zero Charge;  $\zeta$ : Zeta Potential; ( $d_z$ ) Equivalent Hydrodynamic Diameter;  $X_a$ : amount of adsorbed arsenic;  $C_e$ : arsenic concentration at equilibrium;  $X_{MAX}$ : Langmuir maximum adsorption capacity;  $K_L$ : Langmuir affinity constant

## ABSTRACT

This work presents a comprehensive picture of As adsorption on a range of soil colloidal particles in comparable conditions of pH and ionic strength to allow a direct comparison of the surface interactions, including surface charging phenomena.

The highest adsorption capacity for arsenite [As(III)] was shown by the iron minerals, with a clear shift in the surface charge. Pure ferrihydrite could retain over  $5.3 \mu\text{mol m}^{-2}$  of As(III); the adsorption density was reduced to  $3.36 \mu\text{mol m}^{-2}$  when ferrihydrite was a covering film on kaolinite surfaces. Goethite adsorbed up to  $2.3 \mu\text{mol m}^{-2}$  but this amount was nearly halved on Al-substituted goethite and was much lower for hematite. Arsenite adsorption on a poorly ordered Al hydroxide was lower than on poorly ordered and crystalline Fe (hydr)oxides and its adsorption on gibbsite, kaolinite and calcite was almost negligible. When arsenate [As(V)] was added, a similar adsorption capacity for surface unit was shown by both Fe and Al minerals and, differently from As(III), As(V) was adsorbed also on kaolinite and calcite. The adsorption of arsenate on all adsorbents and of arsenite on Fe minerals were observed to be exothermic reaction. The differences in the affinity for As(III) and As(V) adsorption shown by the different soil components were explained in terms of differences in Lewis hardness/softness of adsorbate and adsorbents. These results provide a comparison between possible adsorbents to be used for remediation, and also to assess the As adsorption capacity of soils from their composition.

**Keywords:** arsenate, arsenite, Fe oxides, Al oxides, kaolinite, calcite, adsorption, zeta potential

## INTRODUCTION

Arsenic is a toxic metalloid widespread in soils and waters, where it mainly occurs in the inorganic forms of arsenate [As(V)] and arsenite [As(III)]. The chemical behavior and bioavailability of As in soil and water environments depend largely on its oxidation states. The oxidation of As(III) to As(V) is a kinetically slow process (Masscheleyn et al., 1991) thus, both forms can be simultaneously found in a wide range of natural environments. At the pH most commonly found in soils arsenate occurs in anionic form ( $\text{pK}_{\text{a}1} = 2.3$ ;  $\text{pK}_{\text{a}2} = 6.8$ ;  $\text{pK}_{\text{a}3} = 11.3$ ) while arsenite is mainly

indissociated ( $pK_{a1} = 9.2$ ;  $pK_{a2} = 12.7$ ). Arsenite is more toxic than arsenate and is more mobile in soil (Bissen and Frimmel, 2003; Fendorf and Kocar, 2009).

The main processes controlling the equilibrium of As at the soil-water interface are adsorption/desorption and precipitation/dissolution reactions. At relatively low concentrations, adsorption is the main factor limiting the mobility of As in soil-water systems. The main adsorbants are variable-charge minerals, in particular oxides and (hydr)oxides of Fe and Al (Livesey and Huang, 1981; Manning and Goldberg, 1997; Violante and Pigna, 2002; Van Herreweghe et al., 2003; Norra et al., 2005). Poorly crystallized oxides, because of their high specific surface, can adsorb greater As amounts than the crystalline forms (De Brouwere et al., 2004). Beside the high affinity surfaces of the oxides, other minerals in the clay fraction of soils such as carbonates and phyllosilicates can also contribute to As adsorption (Goldberg and Glaubig, 1988, Goldberg, 2002; Ladeira and Ciminelli, 2004), due to their abundance. The widespread presence of (hydr)oxides precipitated on the surface of soil phyllosilicates, moreover, can strongly modify their reactivity toward As (Martin et al., 2009).

The implications of the surface charging phenomena involved in As adsorption on different substrates have been seldom taken into consideration. Anion adsorption is favored on positively charged surfaces and, as the coverage of the surfaces by anionic adsorbates proceeds, the net negative charge increases, shifting the point of zero charge (PZC) of the mineral particles toward lower pH values and hampering the further adsorption of anions. Shifts in PZC have been considered diagnostic of the formation of inner-sphere complexes with As species on Fe and Al oxides (Sun and Doner, 1996; Jain et al., 1999; Goldberg and Johnston, 2001, Sherman and Randal, 2003, Weerasoorya et al., 2004; Antelo et al., 2005), whereas arsenite is reported to form both inner- and outer-sphere complexes on (hydr)oxides surfaces (Arai et al., 2001; Goldberg and Johnston, 2001). The effects of anion adsorption on the surface charge of the colloids may have important environmental consequences, including the dispersion of colloidal particles in soils and waters. The effects of arsenite and arsenate adsorption on charging phenomena should be taken into consideration for assessing the mobility of As in particulate form. This form can be substantial, reaching 70% of the total As in well water samples (Le, 2002). Unfortunately, the information on charging phenomena linked to As adsorption are sparingly available, especially for As(III), and they concern only a few adsorbent-adsorbate systems.

Many aspects of adsorption of arsenate and, to a lesser extent, of arsenite on several pure minerals representative of the most important As adsorbing phases in soil environments have been studied (Table 1). Most works, however, only consider adsorption on a single or few substrates while studies comparing As adsorption properties of a wide range of different minerals (e.g., Violante and

Pigna, 2002) commonly consider one single As species. In addition, the experiments are often run under different conditions (e.g., adsorption time, temperature, pH, ionic strength). From Table 1 it can be noticed that, although goethite-As is one of the simplest and most studied adsorption systems, the results vary widely, e.g., for As(III) Dixit and Hering (2003) found an adsorbed amount of  $173 \mu\text{mol g}^{-1}$ , while Ladeira et al. (2004) found an amount of  $7.5 \text{ mg g}^{-1}$ , corresponding to nearly  $100 \mu\text{mol g}^{-1}$ ; however a direct comparison is not possible, because one is a synthetic and one a natural oxide, the pH and ionic strength are different, and most probably also the specific surface area differs. The adsorption data of As(V) on goethite found by Liu et al. (2001) are comparable with those reported by Violante and Pigna (2002) at the same pH, while those by Ladeira et al (2004) on a natural goethite are lower; even more evident is the difference between the values of adsorption for surface unit reported by Gimenez et al. (2007) ( $3.0 \times 10^{-6} \text{ mol m}^{-2}$ ) and Silva et al. (2010) ( $4.9 \times 10^{-6} \text{ mol m}^{-2}$ ), possibly due to the different pH. When considering the other adsorbents the differences are much enhanced, especially for the scarcely crystalline ones.

As a consequence, not only a direct comparison of the behavior of the two As species is hindered, but also a comparison of the same species on different soil components, such as Fe and Al (hydr)oxides, making very difficult the elaboration of effective models of the behavior of arsenite and arsenate in soil system.

Aim of this work was to present a complete picture of As adsorption on the most important adsorbants in soils in comparable conditions of pH and ionic strength. To achieve this objective, surface charging phenomena and dispersion-flocculation behavior, in addition to the common adsorption parameters, were taken into proper account. A set of comparable adsorption parameters would eventually lead to a better prediction of the environmental fate of both arsenite and arsenate in the soil-water system.

## **MATERIALS AND METHODS**

Crystalline Fe and Al (hydr)oxides (hematite, pure and Al substituted goethite, gibbsite); short-range ordered Fe and Al (hydr)oxides (pure ferrihydrite and ferrihydrite precipitated on kaolinite, amorphous Al (hydr)oxide); phyllosilicates (kaolinite) and calcite were used for this study.

### Mineral adsorbents

**Crystalline** and **short-range ordered Fe (hydr)oxides** were synthesized in the laboratory according to Schwertmann and Cornell (1991). **Hematite** was obtained by heating 2 L of  $0.002 \text{ M HNO}_3$  to  $98^\circ\text{C}$  and adding 16.6 g of  $\text{Fe}(\text{NO}_3)_3 \cdot 9\text{H}_2\text{O}$  under stirring. The solution was kept

for 7 days at 98°C. For the synthesis of pure **goethite**, 180 mL of 5 M KOH were added to 100 mL of 1 M Fe(NO<sub>3</sub>)<sub>3</sub>, the volume brought to 2 L with deionized water in polyethylene bottles and aged at 70°C for 60 hours. For the **Al-substituted goethite**, 120 mL of a 0.5 M Al(NO<sub>3</sub>)<sub>3</sub> solution were mixed with 165 mL of 5M KOH and 100 mL of a 1M Fe(NO<sub>3</sub>)<sub>3</sub> solution were added under constant stirring in polyethylene flasks. The precipitation product was aged at 70°C for 14 days, then washed with 1 M KOH, and the pH was adjusted at 7.5. The degree of Al-substitution was found to be 10% after chemical analysis. **Two-lines ferrihydrite** was obtained by slowly titrating a 0.2 M Fe(NO<sub>3</sub>)<sub>3</sub> solution to pH 7.5 with 1M KOH.

The **short-range ordered Al oxide** was synthesized according to the method described by Goldberg et al. (2001). Five hundred mL of a 0.408 M AlCl<sub>3</sub> solution were slowly mixed with the same amount of 1.088 M NaOH solution to obtain an Al/OH molar ratio of 0.37. After 15 minutes the precipitate was washed with deionized water. The XRD analysis confirmed the formation of an amorphous precipitation product.

**Gibbsite** was obtained by slowly titrating 0.1 M Al(NO<sub>3</sub>)<sub>3</sub> by 0.5 M NaOH to pH 7.0. The suspension was aged for 7 days at room temperature and then for 20 days at 65°C. At the end of that period the suspension was washed twice with 0.1M HCl to remove the amorphous Al, dialyzed against deionized water and freeze dried (Violante and Pigna, 2002). The formation of pure gibbsite was confirmed by X-ray diffractometry (XRD).

**Calcite** derived from a limestone was ground to less than 2 µm. Main impurities were Mg (0.52%), Si (75 µg g<sup>-1</sup>), Al (58 µg g<sup>-1</sup>), and Fe (36 µg g<sup>-1</sup>). The X-ray diffraction pattern showed the typical pattern of calcite (Celi et al., 2000).

**Kaolinite** (KGa2) was obtained from the Clay Mineral Society. The <2 µm particle size fraction was separated by dispersion at pH 8.5, followed by repeated sedimentation and decantation. This fraction was K-saturated by shaking three times with 1M KCl, and then dialyzed against deionized water until the water was Cl<sup>-</sup> free.

The mixed system **KGa2-Fh** was synthesized by adding a FeCl<sub>3</sub> solution to a kaolinite suspension and slowly titrating to pH 7.5 with 1M KOH. The concentration of the FeCl<sub>3</sub> solution was calculated in order that the ferrihydrite represented 10% (w/w) of the mixed system, i.e. a nearly complete coverage on the kaolinite surfaces (Martin et al., 2009). All the precipitation products were dialyzed. The identity and purity of the obtained iron oxides and the absence of crystalline forms in the mixed system was confirmed by XRD and by the Fe oxalate/total Fe ratio.

The crystalline oxides were freeze-dried after dialysis, while the amorphous Al hydroxide, ferrihydrite, kaolinite and the mixed system kaolinite-ferrihydrite were used as suspensions and an aliquot was freeze dried for the determination of the specific surface.

The specific surface area (SSA) of the crystalline minerals was determined with the BET method by N<sub>2</sub> adsorption (Sorptomatic 1900, Fison Instruments) while the specific surface of the short-range ordered Al hydroxide was determined gravimetrically after water adsorption.

The surface charge of the minerals was measured through a range of pH values to assess the PZC. Aliquots were taken from suspensions of the minerals and their pH was adjusted with HCl or KOH to obtain a range of 3-11, and the electrophoretic mobility of the particles in the suspension was measured by Laser Doppler Velocimetry (LDV-PCS - DELSA 440, Beckman, Coulter Electronics). The electrophoretic mobility data were converted to zeta potential ( $\zeta$ ) using the Smoluchowski equation (Hunter, 1988). The Doppler shift arising from Brownian motion can be used to calculate the average diffusion coefficient of particles, which is converted to an equivalent hydrodynamic diameter ( $d_z$ ) using the Stokes-Einstein equation. All measurements were run in triplicate. Previous experiments (Ajmone Marsan et al., 1997) have demonstrated that this procedure produces reproducible results. The pH was measured potentiometrically.

#### Arsenic solutions

Arsenite and arsenate 1000  $\mu\text{g mL}^{-1}$  stock solutions were obtained by dissolving arsenate or arsenite salts ( $\text{Na}_2\text{HAsO}_4 \cdot 7\text{H}_2\text{O}$ , or  $\text{NaAsO}_2$ , J.T. Baker Chemicals Co, Phillipsburg, NJ, USA) in 0.01 M KCl. Working solutions with concentration of 100 and 10  $\mu\text{g mL}^{-1}$  were prepared by dilution in 0.01 M KCl before use, and the pH was adjusted to 6.5 with HCl. The arsenite containing solutions were prepared and stored under N<sub>2</sub> atmosphere. The absence of oxidation of As(III) to As(V) was tested before each use.

#### Arsenic-minerals interaction

Before the interaction, all the adsorbents were pre-equilibrated in 0.01M KCl for 24 hours at pH 6.5 except for calcite which was equilibrated at a pH around 8 to prevent dissolution.

The concentrations of the mineral suspensions were selected in order to have comparable adsorbing surface in terms of  $\text{m}^2$ . Five mL of each suspension were pipetted in polyethylene test tubes; arsenite or arsenate solutions at suitable concentrations were added to a 10 mL final volume, in order to obtain increasing As concentrations until around the maximum adsorption capacity of each adsorbent, as determined from preliminary tests. The samples were then equilibrated for 24 hours on a reciprocating shaker at 25°C in the dark.

At the end of the interaction period the electrophoretic mobility and the particle size were measured on aliquots of the suspension.

### Isothermal Titration Calorimetry (ITC)

Isothermal titration calorimetric measurements of arsenite or arsenate adsorption were performed on goethite and gibbsite, as representative of crystalline Fe and Al oxides respectively, and on the amorphous Al hydroxide. The measurements performed on ferrihydrite and KGa2-Fh were previously reported by Martin et al. (2009). The titration experiments were performed at 298 K, with a calorimeter ITC 4200 (Calorimetry Sciences Corporation, Lindon, UT, USA) equipped with 1.30 mL cells. The concentration of the adsorbent suspension was 5 mg mL<sup>-1</sup> for goethite and gibbsite and 0.5 mg L<sup>-1</sup> for the short-range ordered Al hydroxide and ferrihydrite. Aliquots of 10 µl of concentrated arsenite or arsenate solutions (in the range 0.8 to 26.6 mM) were injected into the stirred suspension (500 rpm). The enthalpies of dilution of the arsenite or arsenate titrant solutions at the concentrations used for the adsorption experiments were measured by carrying out injection cycles in the absence of the adsorbent.

### Arsenite and arsenate determination.

After centrifugation, the supernatant was filtered through 0.2 µm syringe filters. Arsenite and arsenate in solution were determined with the molybdenum blue colorimetric method as described by Huang and Fujii, (1996). The absorbance of the solution was determined by UV-VIS spectrometry (Hitachi U 2000).

The amount of adsorbed As,  $X_a$ , in µmol As g<sup>-1</sup>, was calculated by the following equation:

$$X_a = [(C_0 - C_e) \cdot V] / m \quad (1)$$

where  $C_0$  is the initial As concentration and  $C_e$  the residual concentration [µmol mL<sup>-1</sup>];  $V$  is the solution volume [mL]; and  $m$  the mass of the adsorbent [g]. The experimental error, estimated after Thomas et al. (1989), was less than 5%.

The adsorption data were fitted to the Langmuir equation in the following form:

$$X_a = X_{MAX} K_L C_e / (1 + K_L C_e) \quad (2)$$

where  $X_{MAX}$  is the maximum amount of As that can bind to the adsorbent (maximum adsorption capacity), and  $K_L$  is an affinity constant. All the experiments were run in duplicate. The parameters obtained with the application of the Langmuir model ( $X_{MAX}$ ,  $K_L$ ) provide useful information about the retention capacity and adsorbent/adsorbate affinity of different adsorbents towards the same adsorbate. In view, however, of the limitations of the application to complex environments such as soils and soil minerals the parameters are to be taken as indicative (Sparks, 2003).

## **RESULTS AND DISCUSSION**

### **Properties of the adsorbent surfaces**

The values of specific surface area (Table 2) were larger for the poorly ordered oxy-(hydr)oxides, while SSA of the crystalline oxides ranged between 40 and 60 m<sup>2</sup>g<sup>-1</sup>. The lowest values were obtained for kaolinite and calcite.

The point of zero charge of all the adsorbents, except hematite and kaolinite, was above pH 6.5 and consequently their surfaces can be considered as positively charged at the pH selected for the adsorption experiments. The size ( $d_z$ ) of the particles of all the minerals was in the range 0.8-1.3  $\mu\text{m}$ . The relatively large particle size obtained for the poorly ordered oxides was attributed to aggregation, although the surfaces were bearing a net positive charge at pH 6.5.

### **Adsorption isotherms**

#### **Arsenite adsorption**

The arsenite adsorption isotherms on all the adsorbents were L-shaped (Dixit and Hering, 2003), except the case of the poorly ordered Al hydroxide (Fig. 1). The fitting of the adsorption data by the Langmuir equation was good ( $r^2 \geq 0.99$ ) for all the iron oxides, while comparatively poor fittings were obtained for arsenite adsorption on Al oxides, kaolinite and calcite (Table 3).

Ferrihydrite (Fig. 1a) showed the highest adsorption capacity toward arsenite and the plateau was not completely reached even at very high adsorbate to adsorbent ratio (nearly 1.7 mmol As g<sup>-1</sup> Fh) in line with the findings of Pierce and Moore (1982) and Raven et al. (1998). The  $X_{\text{MAX}}$  value, although very high, was compatible with adsorption processes (Sverjenski and Fukushima, 2006), and surface adsorption could be the dominating interaction mechanism with ferrihydrite. However, other mechanisms beside adsorption, such as surface precipitation cannot be ruled out. In some studies, as in the present one, the adsorption plateau was not found and that has been explained with surface precipitation, or formation of an arsenite-Fe oxide mixed phase (Raven et al., 1998; Muller et al., 2010). Ferrihydrite has a short-range ordered structure, with nanometric particle size and greater amount of structural defects compared with the crystalline Fe oxides (Smith et al., 2012), hence the nanoparticle effect could contribute to justify the great amount of arsenite adsorbed (Charlet et al., 2011). In soil environments ferrihydrite is often precipitated as a covering film on particles such as phyllosilicates so the nanosize effect could be limited. Indeed, when ferrihydrite

was precipitated on kaolinite surfaces (KGa2-Fh), the adsorption plateau was reached (Fig.1a) and the number of moles of arsenite adsorbed for surface unit decreased. However, considering that ferrihydrite represented 10% (w/w) of the system, the adsorption maxima for mass unit was comparable, in the order of 1.6 mmol As(III) g<sup>-1</sup> of ferrihydrite, and also the K<sub>L</sub> value remained very close to that of pure ferrihydrite (Table 3), suggesting that kaolinite did not substantially affect the arsenite-ferrihydrite interaction.

Arsenite adsorption on the short-range ordered Al hydroxide did not reach saturation (Fig. 1a); the X<sub>a</sub> vs. C<sub>e</sub> plot was better fitted by a straight line (r<sup>2</sup> = 0.957) than by the Langmuir model (r<sup>2</sup> = 0.855) (Table 3) and above C<sub>e</sub> > 0.2 μmol mL<sup>-1</sup> the adsorption isotherm became almost completely linear (r<sup>2</sup> = 0.992; p < 0.005). This behavior is characteristic of C-type isotherms, indicating a non-specific interaction and scarce adsorbent/adsorbate affinity (Sparks, 2003), as confirmed by the very low K<sub>L</sub> value (Table 3). The Al hydroxide used in this experiment adsorbed more arsenite per mass unit than all the crystalline adsorbents (Fig. 1 and Table 3). The adsorption density (μmol m<sup>-2</sup>) per surface unit, on the contrary, appeared to be lower than most of the crystalline Fe oxides, although the comparison is not straightforward because of the different method used for determining the surface area (Table 2).

The adsorption capacity of short-range ordered aluminum oxides toward arsenite is generally reported to be lower than that of iron oxides (Goldberg and Johnston, 2001), resulting in a low effectiveness of Al-based As removal systems when As(III) is involved.

Among the crystalline oxides, pure goethite showed the highest adsorption capacity and affinity for arsenite (Table 3), in line with previous works (Table 1). The adsorption density on the Al-substituted goethite was nearly one half of that on the pure goethite, as well as the K<sub>L</sub> value (Table 3). This lowering in the adsorption density is in agreement with the results of Masue et al. (2007), who found a reduced adsorption on coprecipitated Al-Fe (hydr)oxides. The maximum As(III) adsorption capacity of hematite was lower than that of goethite in terms of both mass and surface unit, and the K<sub>L</sub> value indicated a lower affinity (Table 3). These results are within the very wide range of different adsorption capacities of hematite towards As(III) that have been reported (Table 1), depending on the differences in the experimental conditions, in particle size and crystal shape of the material, natural or synthesized according different procedures.

The adsorption of arsenite on gibbsite, kaolinite and calcite (Fig. 1 and Table 3) was almost negligible if compared to its retention on iron oxides. The scarce capacity of gibbsite to remove As(III) from the solution was substantiated by a very low adsorption density and a K<sub>L</sub> value smaller

than those of all Fe oxides. This is in line with the findings of Weerasoorya et al. (2003) whereas higher As(III) adsorption was reported by Ladeira et al. (2004). In the latter study the presence of Fe impurities in the gibbsite of natural origin might have contributed to enhance As(III) retention.

Similarly to gibbsite, the arsenite adsorption on kaolinite was much lower than that on all Fe-containing adsorbents, with small amounts in agreement with those reported in previous studies, even smaller than  $0.1 \mu\text{mol m}^{-2}$  (Manning and Goldberg, 1997; So et al., 2008). The work of Yokoyama et al. (2012) confirmed the limited adsorption of As(III) on calcite, that is probably combined with As oxidation, since only As(V) was detected on the calcite surfaces after interaction with an As(III) solution.

### **Arsenate adsorption**

Arsenate was always adsorbed with L-shaped isotherms (Fig. 1) with good ( $r^2 > 0.98$ ) fittings of its adsorption data to Langmuir equation (Table 3). Ferrihydrite (Fig. 1b) showed a high adsorption capacity toward arsenate and, similarly to As(III), the association of ferrihydrite with KGa-2 on As(V) adsorption, caused only a slight decrease of the amount of adsorbate retained for surface unit. The mineral association, hence, seemed not to eliminate the nanoparticle effect enhancing the adsorption characteristics of nanoscale adsorbents (Charlet et al., 2011). This observation could have positive implications for the functionality of nano-sized sorbents fixed on coarser supports for the development of As-removal technologies.

The poorly ordered Al hydroxide retained larger amount of arsenate than ferrihydrite for mass unit, with a comparable adsorption density for surface unit, although with a lower  $K_L$  value, confirming the good potential of Al (hydr)oxides for the sequestration of As in the pentavalent form.

Arsenate adsorption on pure goethite was in agreement with the literature reporting adsorbed amounts around  $2.2\text{-}2.5 \mu\text{mol m}^{-2}$  at pH below neutrality, decreasing with increasing alkalinity (Liu et al., 2001; O'Reilly et al., 2001; Violante and Pigna, 2002; Antelo et al., 2005), and the high  $K_L$  value confirmed the great affinity of goethite for arsenate adsorption. Arsenate adsorption density for surface unit on Al-goethite was nearly halved compared with pure goethite, as found for arsenite; however, in contrast with arsenite, the higher  $K_L$  value suggested a greater affinity for arsenate adsorption on the Al-substituted goethite (Table 3).

The arsenate adsorption maxima on hematite were intermediate between goethite and Al-goethite, with the lowest affinity among the Fe oxides, as observed for arsenite adsorption, possibly also in relationship with the low PZC of the substrate. The reactivity of hematite toward As species (Table

1) and, in general, toward anion adsorption at a given pH can vary widely depending on SSA, PZC and crystal shape of the mineral (Venema et al., 1998); moreover, the fact that As(V) forms both inner- and outer-sphere complexes on hematite (Catalano et al., 2007), may further increase the variability in the adsorption capacity of hematites.

As observed for the short-range ordered Al hydroxide, the adsorption capacity of gibbsite toward arsenate was markedly higher than that shown toward arsenite, and was comparable to that of the crystalline Fe (hydr)oxides. Differently from arsenite, arsenate was adsorbed also on kaolinite and calcite (Fig. 1), with comparable adsorption density and affinity between the two solids (Table 3). Clay phyllosilicates could represent an As sink in soils because of their large amount, in particular kaolinitic minerals displaying relatively large amounts of variable-charge sites. However, arsenate seems to be weakly retained on kaolinite surface, despite some observed inner-sphere bonding with the octahedral aluminum, possibly co-existing with outer-sphere interaction (Arai, 2010).

In spite of its low As adsorption capacity, calcite can play a relevant role in As adsorption (Goldberg and Glaubig, 1988) and As removal from the solution could be expected, in addition to adsorption, for the possible formation of surface precipitates (Roman-Ross et al., 2006).

Thus, differently from As(III), when As was added as As(V), the adsorption capacity of Fe and Al oxides are comparable (Fig. 1 and Table 3), for both the poorly ordered and the well crystallized forms. The adsorption maxima were still much greater for the poorly ordered materials compared with the crystalline ones, but for As(V) they varied in a smaller range and the adsorption plateau was reached also in the cases of ferrihydrite and short-range ordered Al-hydroxide. The Langmuir constant,  $K_L$ , clearly showed a higher affinity of both As species to the iron-containing substrates (with the exception of hematite) than to the other minerals. The differences in the adsorption capacities toward As(III) and As(V) were smaller for the Fe oxides and much bigger for all the other minerals, as evidenced by the As(III)/As(V) adsorption ratios (Table 3). The  $K_L$  values, always higher for As(V) than for As(III), indicated that the former was always adsorbed with higher affinity, even where the latter was retained in greater amounts.

### **Effect on pH, surface charge and particle size**

The specific adsorption of anionic species is known to affect the surface charge of colloidal particles and the pH of the solution contrary to nonspecific adsorption phenomena (Hunter, 1986). The measure of the electrophoretic mobility, and the pH variations induced by adsorption, may hence supply an indirect, but easy to obtain, indication on the adsorption mechanism. If an increase of the negative surface charges and solution pH was expected after As(V) adsorption on most

substrate, the effect of As(III), prevalently uncharged at the experimental pH, was harder to predict, although a shift in the surface charge towards more negative values was observed for As(III) adsorption on short-range ordered Fe oxides (Jain et al., 1999; Goldberg and Johnston, 2001).

### Arsenite

The formation of inner-sphere complexes is the main mechanism proposed for arsenite adsorption on most Fe (hydr)oxides (e.g. Manning et al., 1998; Ona-Nguema et al., 2005), possibly combined with outer-sphere adsorption, accordingly with the characteristics of the solid surface and the experimental conditions (Stachowicz et al., 2006; Sverjensky and Fukushi, 2006).

The adsorption of arsenite on ferrihydrite induced a pH decrease, in line with the observations by Jain et al. (1999). The same effect was here observed for all the iron oxides while the pH was not affected by the As(III) interaction with the other minerals (Fig. 2). At pH 6.5, the mineral surfaces were mostly positively charged (Table 2), except those of kaolinite and hematite. The increase of surface coverage with arsenite caused a shift of the  $\zeta$  potential (Fig.3) towards more negative values when iron was the adsorbing phase. The net positive charge (+22 mV) of ferrihydrite surfaces at pH 6.5 gradually decreased, finally reaching negative values, as the arsenite adsorption proceeded. The drop in the net positive surface charge was even more evident when ferrihydrite was precipitated with kaolinite, with reversal of the sign of the surface charge at nearly 50% of the surface coverage. For goethite, 75% surface coverage was needed to obtain a net negative charge (-7.5 mV), and the same shift in the  $\zeta$  potential was observed for Al-goethite. On the contrary, with all the adsorbents that did not contain Fe, the net surface charge remained almost unvaried.

The shift of the  $\zeta$  potential towards negative values after arsenite adsorption on Fe-based adsorbents is in agreement with what has been reported for goethite (Luxton et al., 2006) and poorly ordered iron oxides (Jain et al., 1999; Goldberg and Johnston, 2001) as indicative of the formation of inner-sphere complexes. The adsorption of neutral species, such as arsenite at pH well below the  $pK_{a1}$ , may result in the introduction of negative charge inside the shear plane when the acid is deprotonated to form the inner-sphere complex (Jain et al., 1999). In fact, such complexes were observed by spectroscopic studies on As(III) adsorption on iron (hydr)oxides (Sun and Doner, 1996; Manning et al., 1998; Ona-Nguema et al., 2005). The negative shift in the  $\zeta$  potential was here observed also for hematite and Al-goethite, indicating that the formation inner-sphere complex could represent the main adsorption mechanism of arsenite when Fe (hydr)oxides are involved.

The almost negligible changes in the  $\zeta$  potential observed after arsenite adsorption on the Al oxides, calcite and kaolinite, (Fig. 3) were consistent with the unchanged pH. These observations support

the hypothesis that the adsorption of arsenite on Al oxides mainly occurs via outer-sphere interaction, and even if inner-sphere complexes are formed (Arai et al., 2001) they are not able to affect the overall surface charge (Goldberg and Johnston, 2001; Weerasooriya et al., 2003). The linear shaped adsorption isotherm of As(III) on the poorly ordered Al-hydroxide, in particular at high As additions (Fig. 1), further supports the prevalence of a non-specific, outer-sphere interaction with this adsorbent. In the case of gibbsite, kaolinite and calcite, even if an inner-sphere complex is formed (Goldberg, 2002; Sverjensky and Fukushi, 2006), the very low adsorption density would imply a hardly detectable charge variation, possibly masked by the experimental uncertainty.

The surface charge variations on colloidal particles are reflected in the dispersion/flocculation behavior of the colloidal suspension. The measure of the average apparent particle size at increasing arsenite coverage on ferrihydrite showed a tendency to particle aggregation (Fig. 4) as the net positive charge of the surface was being neutralized by arsenite coverage and a re-dispersion after the charge reversal. A similar behavior, although less evident, can be observed for the KGa2-Fh system, as well as for the crystalline Fe (hydr)oxides. Also the poorly ordered Al hydroxide showed a rapid aggregation at low As(III) concentration, then the particle size returned at the values measured for this substrate at pH 6.5 in the absence of As(III). Gibbsite, kaolinite and calcite particle size was not clearly affected by As(III) adsorption

### Arsenate

Arsenate adsorption on all the tested minerals induced a clear pH increase (Fig. 2) as expected for the specific adsorption of oxyanions substituting the hydroxyl ions of the surfaces. When As(V) was added, the shift of  $\zeta$  potential toward more negative values was evident for all the adsorbents and always more pronounced than in the case of arsenite (Fig.3). The shift in  $\zeta$  potential of all iron oxides is indicative of inner-sphere interaction, similarly to phosphate adsorption (Celi et al., 1999). A charge reversal was induced on the surfaces of the iron oxides. The starting  $\zeta$  potential of goethite, for instance, was +20 mV; this positive charge was neutralized by an As(V) coverage of the surface as low as 5-10%, and the charge reversal (-20 mV) was obtained at 40% surface coverage. These results match with a prevalence of inner-sphere complex formation and indeed bidentate, binuclear bonding of As(V) to the goethite surface has been detected by EXAFS spectroscopy (Waychunas et al., 1993; Farquhar et al., 2002; Sherman and Randall, 2003). Model calculations by Fukushi and Sverjensky (2006) indicated that the binuclear bidentate complex would be increasingly deprotonated with increasing pH, thus explaining the drastic changes in  $\zeta$  potential. The mechanism appears to be similar to that of the adsorption of phosphate (Goldberg and

Johnston, 2001), involving the replacement of two contiguous hydroxyl groups singly coordinated to two ferric ions. This is confirmed by the value for As(V) adsorption capacity of  $2.5 \mu\text{mol m}^{-2}$  which is analogous to the phosphate adsorption on goethite (Torrent et al., 1990; Venema et al., 1998).

A negative shift in the  $\zeta$  potential was also observed for hematite. Also for this Fe oxide inner-sphere complexes with As(V) have been detected (Waychunas et al., 2005), with the possible simultaneous presence of outer-sphere complexes (Catalano et al., 2007). Arsenate adsorption induced detectable shifts in the  $\zeta$  potential accompanied with pH increase also for kaolinite and calcite, confirming inner-sphere adsorption with ligand exchange also for these minerals.

The less pronounced changes in the  $\zeta$  potential induced by arsenite compared to arsenate adsorption is clearly linked to the different  $\text{pK}_a$  of arsenous and As acids: at pH 6.5 a mostly neutral species were adsorbed in the former case, while in the latter the surfaces were covered with well dissociated anionic species. The pH increase induced by arsenate adsorption (Fig. 2), moreover, further enhanced the shift of the  $\zeta$  potential toward more negative values, while arsenite adsorption reaction is proton releasing at  $\text{pH} < \text{pK}_a^1$  for  $\text{H}_3\text{AsO}_3$  and the induced lowering of the pH partly opposed the development of net negative charge on the surfaces.

In general, aggregation was observed as arsenate adsorption neutralized the net positive charge of the surface, until reaching the PZC of the oxides; then, dispersion of the colloidal particles was observed at high arsenate loading, as a consequence of the induced high net negative charge (Fig. 4). Gibbsite, that remained positively charged along the whole As(V) adsorption isotherm, only showed a progressive aggregation while approaching surface neutralization, while no specific trend was observed in the particle size after arsenate adsorption on KGa2-Fh, kaolinite and calcite.

Several authors reported the predominance of inner-sphere adsorption of arsenate on both crystalline or short-range ordered aluminum oxides (Manning and Goldberg, 1996; Arai et al., 2001; Goldberg and Johnston, 2001; Weerasooriya et al., 2004). The shifts in the surface charge observed on arsenate adsorption support the formation of an inner-sphere complex, although the observed changes are less pronounced than with Fe oxides. In the case of gibbsite, the charge is positive along the whole adsorption isotherm. A binuclear, bidentate complex was found to be the dominant mechanism (Arai et al., 2001; Ladeira et al., 2001; Fukushi and Sverjensky, 2006). The amount of As(V) adsorbed on kaolinite is comparable to the loadings found in literature (Ladeira et al. 2004; Quaghebeur et al., 2005), or lower (Violante and Pigna, 2002). Kaolinite can adsorb arsenate via ligand exchange on the active aluminol groups at the crystal edges and the formation of

an inner-sphere complex is supported by model calculation (Goldberg and Glaubig, 1988; Goldberg, 2002). The adsorption of arsenate on calcite is reported to be important in soils mainly at high pH.

### **ITC measurements**

The measured heat of adsorption is the result of the combination of different chemical processes and, for this reason, only the overall  $\Delta H$  was obtained from the calorimetric measurements. The energy of reaction for the same adsorbent/adsorbate system can actually vary according to the type of surface complex formed and surface charge. Kwon and Kubicki (2004) reported that the calculated heat of adsorption of phosphate on iron oxides could be either endothermic or exothermic, ranging between +30 and -61 kJ mol<sup>-1</sup>, according to the reaction conditions and kind of As-surface bonding formed. The experimental conditions were here chosen in order to allow at least a comparison of values obtained for the different adsorbent/adsorbate systems. The heats of adsorption of As(III) on the Fe (hydr)oxides (Table 4) were comparable and less negative than those obtained for As(V) adsorption (ranging from -24.4 to -32.9 kJ mol<sup>-1</sup> for As(III) adsorption and from -39.9 to -45.1 kJ mol<sup>-1</sup> for As(V) adsorption). The heat of adsorption of As(V) on the Al (hydr)oxides was always negative as well (-21.6 and -28.8 kJ mol<sup>-1</sup> for the short-range ordered Al hydroxide and gibbsite respectively), although with smaller absolute values than those obtained for the Fe (hydr)oxides. The heat of adsorption of arsenite on the Al (hydr)oxides, on the contrary, gave slightly positive and poorly replicable values. The negative values for arsenate adsorption on all adsorbents and for arsenite adsorption on the Fe (hydr)oxides obtained under our experimental conditions indicate an overall exothermic reaction in each of these reaction system. The scarcely replicable and slightly positive results obtained for arsenite adsorption on the Al (hydr)oxides suggest an overall entropy-driven phenomenon. The simultaneous occurrence of some exothermic adsorption reactions, however, cannot be ruled out, their effect possibly being masked within the overall phenomenon.

### **Adsorption of As according to HSAB theory**

Considering the *Hard and Soft Acids and Bases* theory (Pearson, 1963) applied to adsorption phenomena on soil colloidal surfaces (Niskanen, 2006) soft Lewis bases would preferentially interact with soft Lewis acids, while hard bases would interact with hard acids. Arsenite, compared to arsenate, is a relatively soft Lewis base, since the unshared electron pair results in a deformable and polarisable electron cloud; Fe atoms, on the other side, with incomplete 3d orbital, is a relatively soft Lewis acid, hence favoring As(III) adsorption on the iron-bearing surfaces (Vatutsina

et al., 2007). On the contrary, Al-based adsorbents, resulting harder Lewis acids, have scarce affinity for As(III), showing a strong selectivity toward harder As(V) anions. Similarly, a lower affinity of relatively soft ligands, such as natural organic matter, for Al-centered versus Fe-centered adsorption site was evidenced (Schnitzer, 1995; Meier et al., 1999). This is also in agreement with the observed greater affinity of the aluminum-based adsorbent toward phosphate compared to arsenate, while the contrary happens in the case of iron-based adsorbents (Violante et al., 2003), being phosphate a harder Lewis base than arsenate. This could be explained with the different acidity of Al oxides compared with Fe oxides. Although Fe is more electronegative than Al, the charge/radius ratio of the trivalent cations is higher for the smaller Al ion, and the acidity of surficial Al in the hydroxide octahedral structure result higher than the acidity of the Fe trivalent ions. This implies a higher reactivity of the hydroxyls on the Fe-(hydr)oxide surface, the ligand exchange with the As oxy-acids resulting easier. The higher acidity of Al in the Al (hydr)oxide also implies higher solvation energy and the hydration water molecules are harder to remove in order to allow the approach of the adsorbate to the surface. The arsenate ion is already dissociated at circum-neutral pH and the electrostatic attraction of the positively charged surface is more effective in enhancing the anion to approach the reactive sites compared to the neutral arsenite molecule. Moreover, additional energy to deprotonate the arsenous acid is needed, and the resulting acidification of the media after arsenite adsorption further hampers the reaction on a more acidic substrate, while the adsorption of arsenate, that causes a pH increase, is favored (Fig. 2). The reaction energies involved probably have a threshold effect causing selectivity toward arsenate adsorption on Al oxides. Thus, due to the intrinsic differences between Fe and Al minerals, both arsenite and arsenate adsorption are comparable on Fe oxides, while on Al oxides only arsenate is adsorbed.

### **Environmental considerations**

The differences in As retention capacities of the different minerals are shown in Table 5, that reports the suspension concentration ( $\text{g L}^{-1}$ ) of each adsorbing mineral needed to keep an equilibrium concentration in solution of 0.05 (or 0.01)  $\text{mg L}^{-1}$  when the solution contains 1  $\text{mg L}^{-1}$  of arsenite or arsenate. These equilibrium concentrations represent respectively the maximum admissible As concentration in drinking water in several As-affected Countries (e.g. Bangladesh, India), or according to the WHO guidelines. The amounts of needed adsorbent can vary from less than 0.1 (or 0.5)  $\text{g L}^{-1}$  for ferrihydrite to kilograms for calcite. The short-range ordered Al hydroxide and gibbsite are effective adsorbents for arsenate only. In the soil system, at circum-neutral pH (not accounting for the competition with other ligands), one  $\text{dm}^3$  of soil should contain more than 1 kg

of calcite, or more than 600 g of gibbsite or 250 g of kaolinite in order to keep a concentration of arsenite in soil solution  $<0.05 \text{ mg L}^{-1}$  when irrigated with water containing  $1 \text{ mg L}^{-1}$  As(III), whereas only 0.1 g of ferrihydrite would be enough to reach the same result.

## CONCLUSIONS

A consistent picture of the relationships between As species and the surface of several common minerals was obtained through a series of standardized experiments. The widely accepted instance assessing the scarcer retention of arsenite compared to arsenate on solid phases is confirmed by our results, when aluminum, phyllosilicates or calcite are important sorbing phases, but it results in itself too simplistic, since Fe oxides are the main As bearing phases in several soils. Arsenite is in fact adsorbed in higher amounts than arsenate on all iron oxides, except at very low concentration. The As retention capacity of soils is related to their content in clay and Fe and Al (hydr)oxides. Soil Fe and Al (hydr)oxides are mostly contained in the finest fractions (clay, fine silt) and they probably account for most of the retention of the clay fraction toward arsenate while Fe (hydr)oxides, in more or less crystalline forms or as coatings on clay minerals, appear to be mostly responsible for the soil adsorbing capacity toward arsenite.

These results may thus provide a tool to assess the As adsorption capacity of soils according to their characteristics and permit a comparison between possible adsorbents to be used for remediation.

## ACKNOWLEDGMENTS

*This study is dedicated to the memory of Dr. P.M. Huang, who inspired this research pathway.*

This research was supported by the Italian Ministry of University and Research (MIUR), PRIN Project. The Isothermal Titration Calorimetry experiments were performed at the Saskatchewan Structural Sciences Center. Dr. J. Maley is gratefully acknowledged for his help in obtaining and interpreting the calorimetric results.

## REFERENCES

- Ajmone Marsan, F., C. Scarnecchia, E. Barberis, and E. Arduino. 1997. Zeta potential of two smectites in the presence of different cations as measured by LDV-PCS. 11th International Clay (AIPEA) Conference. Ottawa (Canada). 15-21 June 1997.
- Alexandratos, V.G., E.J. Elzinga, R.J. Reeder. 2007. Arsenate uptake by calcite: Macroscopic and spectroscopic characterization of adsorption and incorporation mechanisms. *Geochim. Cosmochim. Acta* 71:4172–4187.
- Anderson, M.A., J.P. Ferguson, and J. Gavis. 1976. Arsenate adsorption on amorphous aluminum hydroxide. *J. Colloid Interface Sci.* 54:391-399.
- Antelo, J., M.Avena, S.Fiol, R.López, and F. Arce. 2005. Effects of pH and ionic strength on the adsorption of phosphate and arsenate at the goethite-water interface. *J. Colloid Interf. Sci.* 285:476-486.
- Arai, Y. 2010. Effect of dissolved calcium on arsenate sorption at the kaolinite-water interface. *Soil Sci.* 175:207-213.
- Arai, Y., E.J. Elzinga and D.L. Sparks. 2001. X-ray adsorption spectroscopic investigation of arsenite and arsenate adsorption at the aluminum oxide-water interface. *J. Colloid Interf. Sci.* 235:80-88.
- Bissen, M. and F.H.Frimmel 2003. Arsenic, a review. Part I: occurrence, toxicity, speciation, mobility. *Acta Hydrochim. Hydrobiol.* 31:9–18.
- Catalano, J.G., C.Park, P.Fenter and Z. Zhang. 2008. Simultaneous inner- and outer-sphere arsenate adsorption on corundum and hematite. *Geochim. Cosmochim. Acta* 72:1986-2004.
- Celi, L., S. Lamacchia, F. Ajmone-Marsan and E. Barberis. 1999. Interaction of inositol hexaphosphate on clays: adsorption and charging phenomena. *Soil Sci.* 164:574-585.
- Celi, L., S. Lamacchia and E. Barberis. 2000. Interaction of inositol phosphate with calcite. *Nutr. Cycl. Agroecosys.* 57:271-277.
- Charlet, L., G. Morin, J. Rose, Y. Wang, M. Auffan, A. Brunol, and A. Fernandez-Martinez. 2011. Reactivity at (nano)particle-water interfaces, redox processes and arsenic transport in the environment. *C. R. Geoscience.* 343:123-139.

- De Brouwere, K., E. Smolders, and R. Merckx. 2004. Soil properties affecting solid-liquid distribution of As(V) in soils. *Eur. J. Soil Sci.* 55:165-173.
- Dixit, S., J.G. Hering. 2003. Comparison of arsenic(V) and arsenic(III) sorption onto iron oxide minerals: implications for arsenic mobility. *Environ. Sci. Technol.* 37:4182-4189.
- Duarte, G., Ciminelli, V.S.T., Dantas, M.S.S., Duarte, H.A., Vasconcelos, I.F., Oliveira, A.F., K. Osseo-Asare. 2012. As(III) immobilization on gibbsite: Investigation of the complexation mechanism by combining EXAFS analyses and DFT calculations. *Geochim. Cosmochim. Acta* 83:205–216.
- Farquhar, M.L., J.M. Charnock, F.R. Livens, and D.J. Vaughan. 2002. Mechanisms of arsenic uptake from aqueous solution by interaction with goethite, lepidocrocite, mackinawite, and pyrite: an X-ray absorption spectroscopy study. *Environ. Sci. Technol.* 36:1757-1762.
- Fendorf, S. and B.D. Kocar. 2009. Biogeochemical processes controlling the fate and transport of arsenic: implications for South and Southeast Asia. *Adv. Agron.* 104:137–164.
- Fukushi, K. and D.A. Sverjensky. 2007. A predictive model (ETLM) for arsenate adsorption and surface speciation on oxides consistent with spectroscopic and molecular evidences. *Geochim. Cosmochim. Acta* 71:3717-3745.
- Gimenez, J., M. Martinez, J. de Pablo, M. Rovira, L. Duro. 2007. Arsenic sorption onto natural hematite, magnetite, and goethite. *J. Hazard. Mater.* 141:575–580.
- Goldberg S. 2002. Competitive adsorption of arsenate and arsenite on oxides and clay minerals. *Soil Sci. Soc. Am. J.* 66:413-421.
- Goldberg S. and C.T. Johnston. 2001. Mechanisms of arsenic adsorption on amorphous oxides evaluated using macroscopic measurements, vibrational spectroscopy and surface complexation modeling. *J. Colloid Interf. Sci.* 234:204-216.
- Goldberg, S., and R. A. Glaubig. 1988. Anion sorption on a calcareous montmorillonitic soil-Arsenic. *Soil Sci. Am. J.* 52:1297- 1300.
- Goldberg, S., I. Lebron, D.L. Suarez and Z.R. Hinedi. 2001. Surface characterization of amorphous aluminum oxides. *Soil Sci. Soc. Am. J.* 65:78-86.
- Hsia, T.H., S.L. Lo, and C.F. Lin. 1992. As(V) adsorption on amorphous iron oxide: triple layer modeling. *Chemosphere* 25:1825-1837.

- Huang, P.M. and R. Fujii. 1996. Methods of soil analysis. Part 3. Chemical methods. SSSA Book series no 5. Madison, WI, USA. pp 793-831.
- Hunter, R.J. 1986. Foundations in colloid science. Vol. I and II. Oxford University Press, New York, USA.
- Hunter, R.J. 1988. Zeta potential in colloid science. Principles and applications. Academic Press. London, UK.
- Kwon, K.D. and J. D.Kubicki 2004. Molecular orbital theory study on surface complex structures of phosphates to iron hydroxides: calculation of vibrational frequencies and adsorption energies. *Langmuir*, 20:9249-9254
- Jain, A.,K.P. Raven and R.H. Loeppert. 1999. Arsenite and arsenate adsorption on ferrihydrite: surface charge reduction and net  $-OH^-$  release stoichiometry. *Environ. Sci. Technol.* 33:1179-1184.
- Ladeira, A.C.Q. and V.S.T. Ciminelli. 2004. Adsorption and desorption of arsenic on an oxisol and its constituents. *Water Res.* 38:2087-2094.
- Le, X.C. 2002. Arsenic speciation in the environment and humans. *In*: W.T. Frankenberger Jr. (ed.) *Environmental chemistry of arsenic*. Marcel Dekker, New York.
- Liu, F., A. De Cristofaro, and A. Violante. 2001. Effect of pH, phosphate and oxalate on the adsorption/desorption of arsenate on/from goethite. *Soil Sci.* 166:197-208.
- Livesey, N.T., and P.M. Huang. 1981. Adsorption of arsenate by soils and its relation to selected chemical properties and anions. *Soil Sci.* 131:88-94.
- Luxton, T.P, C.J.Tadanier, and M.J.Eick. 2006. Mobilization of arsenite by competitive interaction with silicic acid. *Soil Sci. Soc. Am. J.* 70:204-214.
- Manning, B.A. and S. Goldberg. 1996. Modeling arsenate competitive adsorption on kaolinite, montmorillonite and illite. *Clay Clay Min.* 44:609-623.
- Manning, B.A. and S. Goldberg. 1997. Adsorption and stability of arsenic (III) at the clay mineral-water interface. *Environ. Sci. Technol.* 31:2005-2011.
- Manning, B.A., S.E. Fendorf, and S. Goldberg. 1998. Surface structures and stability of arsenic(III) on goethite: spectroscopic evidence for inner-sphere complexes. *Environ. Sci. Technol.* 32:2383-2388.

- Manning, B.A., M.L. Hunt, C. Amrhein, and J. Yarmoff. 2002. Arsenic(III) and arsenic(V) reactions with zerovalent iron corrosion products. *Environ. Sci. Technol.* 36:5455-5461.
- Martin, M., L. Celi, E. Barberis, A. Violante, L. M. Kozak, and P. M. Huang. 2009. Effect of humic acid coating on arsenic adsorption on ferrihydrite-kaolinite mixed systems. *Can. J. Soil Sci.*, 89:421-434.
- Masue, Y., R.H. Loeppert and T.A. Kramer. 2007. Arsenate and arsenite behavior on coprecipitated aluminium:iron hydroxides. *Environ. Sci. Technol.* 41:837-842.
- Masscheleyn, P.H., R.D. Delaune and W.H. Patrick, Jr. 1991. Effect of redox potential and pH on arsenic speciation and solubility in a contaminated soil. *J. Environ. Qual.* 25:1414-1419.
- Meier, M., K. Namjesnik-Dejanovic, P.A. Maurice, Y.P. Chin and G.R. Aiken. 1999. Fractionation of aquatic natural organic matter upon sorption to goethite and kaolinite. *Chem. Geol.*, 157:275-284.
- Muller, K., V.S.T. Ciminelli, M.S.S. Dantas, and S. Willscher. 2010. A comparative study of As(III) and As(V) in aqueous solution and adsorbed on iron oxy-hydroxides by Raman spectroscopy. *Water Res.* 44:5660-5672.
- Niskanen R. 2006 Lewis acid-base concept – a unifying principle applicable to soil system, geochemistry and biology. *J. Food Agric. Environ.*, 4:197-201.
- Norra, S., Z.A. Berner, P. Agarwala, F. Wagner, D. Chandrasekharam, and D. Stuben. 2005. Impact of irrigation with As rich groundwater on soil and crops: a geochemical case study in West Bengal Delta Plain, India. *Applied Geochem.* 20:1890-1906.
- O'Reilly, S.E., D.G. Strawn and D.L. Sparks. 2001. Residence time effect of arsenate adsorption/desorption mechanisms on goethite. *Soil Sci. Soc. Am. J.* 65:67-77.
- Ona-Nguema, G., G. Morin, F. Juillot, G. Calas, and G. E. Brown jr. 2005. EXAFS analysis of arsenite adsorption onto two-line ferrihydrite, hematite, goethite, and lepidocrocite. *Environ. Sci. Technol.* 39:9147-9155.
- Pearson, R.G. 1963. Hard and Soft Acids and Bases. *J. Am. Chem. Soc.* 85:3533–3539.
- Pierce, M.L., and C.B. Moore 1982. Adsorption of arsenite and arsenate on amorphous iron hydroxide. *Water Res.* 16:1247-1253.
- Quaghebeur, M., A. Rate, Z. Rengel, and C. Hinz 2005. Desorption kinetics of arsenate from kaolinite as influenced by pH. *J. Environ. Qual.* 34:479-486.

- Raven, K., A. Jain, and R. H. Loeppert. 1998. Arsenite and arsenate adsorption on ferrihydrite: kinetics, equilibrium, and adsorption envelopes. *Environ. Sci. Technol.* 32: 344-349.
- Roman-Ross, G., G.J. Cuello, X. Turrillas, A. Fernández-Martínez, and L. Charlet, 2006. Arsenite sorption and co-precipitation with calcite. *Chem. Geol.*, 233:328–336.
- Schnitzer, M., 1995. Organic-inorganic interactions in soils and their effects on soil quality. In: *Environmental impact of soil component interactions. Natural and anthropogenic organics.* P.M. Huang, J. Berthelin, J.M. Bollag, W.B. McGill and A.L. Page Eds. Lewis Publishers, Boca Raton, USA.
- Schwertmann, U. and R.M. Cornell. 1991. *Iron oxides in the laboratory. Preparation and characterization*, VCH, Weinheim.
- Sherman, D.M. and S.R. Randall. 2003. Surface complexation of arsenic(V) to iron(III) (hydr)oxides: structural mechanism from ab initio molecular geometries and EXAFS spectroscopy. *Geochim. Cosmochim. Acta* 67:4223-4230.
- Silva, J., J.W.V. Mello, M. Gasparon, W.A.P. Abrahao, V.S.T. Ciminelli, T. Jong. 2010. The role of Al-Goethites on arsenate mobility. *Water Res.* 44:5684-5692.
- Singh, D.B., Prasad, G. Rupainwar, D.C. and Singh, V.N. 1988. As(III) removal from aqueous solution by adsorption. *Water Air Soil Poll.* 42:373-386
- Smith, S.J., K. Page, H. Kim, B.J. Campbell, J. Boerio-Goates, and B.F. Woodfield. 2012. Novel synthesis and structural analysis of ferrihydrite. *Inorg. Chem.* 51:6421–6424.
- So, H.U., D. Postma, R. Jakobsen and F. Larsen. 2008. Sorption and desorption of arsenate and arsenite on calcite. *Geochim. Cosmochim. Acta* 72:5871–5884.
- Sparks, D.L. 2003. *Environmental soil chemistry*. II edition. Academic Press, San Diego (CA), USA.
- Stachowicz, M., T. Hiemstra, W.H. van Riemsdijk. 2006. Surface speciation of As(III) and As(V) in relation to charge distribution. *J. Colloid Interf. Sci.* 302:62–75.
- Sun, X., and H.E. Doner. 1996. An investigation of arsenate and arsenite bonding structures on goethite by FTIR. *Soil Sci.* 161:865-872.
- Sverjensky, D.A. and K. Fukushi. 2006. A predictive model (ETLM) for As(III) adsorption and surface speciation on oxides consistent with spectroscopic data. *Geochim. Cosmochim. Acta* 70:3778-3802.
- Thomas, F., J.Y. Bottero and J.M. Cases. 1989. An experimental study of the adsorption mechanisms of aqueous organic acids on porous aluminas. 1. The porosity of the adsorbent: a determining factor for the adsorption mechanisms. *Colloid Surf.* 37:269-280.

- Torrent, J., V. Barron and U. Schwertmann. 1990. Phosphate adsorption by goethites differing in crystal morphology. *Soil Sci. Soc. Am. J.* 54:1007-1012.
- Van Herreweghe, S., R.Swennen, C. Vandecasteele, and V.Cappuyns. 2003. Solid phase speciation of arsenic by sequential extraction in standard reference materials and industrially contaminated soil samples. *Environ. Pollut.* 122:323–342.
- Vatutsina, O.M., V.S.Soldatov, V.I.Skolova, J.Johann, M.Bissen, and A. Weissenbacher.2007. A new hybrid (polymer/inorganic) fibrous sorbent for arsenic removal from drinking water. *React. Funct. Polym.* 67: 184-201.
- Venema, P., T. Hiemstra, P.G. Weidler, and W.H. van Riemsdijk. 1998. Intrinsic proton affinity of reactive surface groups of metal (hydr)oxides: application to iron (hydr)oxides. *J. Colloid Interf. Sci.* 198:282-295.
- Violante, A., and M. Pigna. 2002. Competitive sorption of arsenate and phosphate on different clay minerals and soils. *Soil Sci. Soc.Am. J.* 66:1788-1796.
- Violante, A., M. Ricciardella, and M. Pigna. 2003. Adsorption of heavy metals on mixed Fe-Al oxides in the absence or presence of organic ligands. *Water Air Soil Pollut.* 145:289-306.
- WaychunasG.A., B.A.Rea, C.C. Fuller, J.A. Davis. 1993. Surface chemistry of ferrihydrite: Part I. EXAFS studies of the geometry of coprecipitated and adsorbed arsenate. *Geochim. Cosmochim. Acta* 57:2251-2269.
- Waychunas, G., T. Trainor, P. Eng, J. Catalano, G. Brown, J. Davis, J. Rogers, and J. Bargar. 2005. Surface complexation studied via combined grazing-incidence EXAFS and surface diffraction: arsenate on hematite (0001) and (10–12). *Anal. Bioanal. Chem.* 383:12–27.
- Weerasooriya, R., H.J.Tobschall, H.K.D.K.Wijsekara, E.K.I.A.U.K.Arachchige, and K.A.S.Pathirathne, 2003. On the mechanistic modeling of As(III) adsorption on gibbsite. *Chemosphere* 51:1001-1013.
- Weerasooriya, R., H.J.Tobschall, H.K.D.K.Wijsekara, A. Bandara. 2004. Macroscopic and vibration spectroscopic evidence for specific bonding of arsenate on gibbsite. *Chemosphere* 55:1259-1270.
- Yokoyama, Y., K. Tanaka, and Y. Takahashi. 2012.Differences in the immobilization of arsenite and arsenate by calcite. *Geochim. Cosmochim. Acta* 91:202–219.

Table 1. Adsorption parameters for As species from the literature

	$X_{MAX}^{\dagger}$	pH	I.S. <sup>‡</sup>	As species	Reference
Goethite	173 $\mu\text{mol g}^{-1}$	8	0.01	As(III)	Dixit and Hering (2003)
	7.5 $\text{mg g}^{-1}$	5.5	0.15	As(III)	Ladeira et al. (2004) <sup>§</sup>
	$(2.5\pm 0.1)\times 10^{-6} \text{ mol m}^{-2}$	7.5		As(III)	Gimenez et al. (2007)
	185.7 $\text{mmol kg}^{-1}$	4.0	0.1	As(V)	Liu et al. (2001)
	193-173 $\text{mmol kg}^{-1}$	4-7	0.05	As(V)	Violante and Pigna (2002)
	12.4 $\text{mg g}^{-1}$	5.5	0.15	As(V)	Ladeira et al. (2004) <sup>§</sup>
	$(3.0\pm 0.2)\times 10^{-6} \text{ mol m}^{-2}$	7.5		As(V)	Gimenez et al. (2007)
	0.101 $\text{mmol g}^{-1}$ ; 0.0049 $\text{mmol m}^{-2}$	5.0	0.01	As(V)	Silva et al. (2010)
Al-Goethite	0.0035-0.0032 $\text{mmol m}^{-2}$	5.0	0.01	As(V)	Silva et al. (2010)
Hematite	2.6 $\mu\text{mol g}^{-1}$	7		As(III)	Singh et al. (1988) <sup>§</sup>
	40 $\text{mg k g}^{-1}$			As(III)	Manning et al. (2002)
	$(9.3\pm 0.2)\times 10^{-6} \text{ mol m}^{-2}$	7.3		As(III)	Gimenez et al. (2007)
	20000 $\text{mg g}^{-1}$	6		As(III)	Luther et al. (2012)
	$(2.9\pm 0.5)\times 10^{-5} \text{ mol m}^{-2}$	7.3		As(V)	Gimenez et al. (2007)
	0.193 $\text{mmol g}^{-1}$ ; 0.0055 $\text{mmol m}^{-2}$	5.0	0.01	As(V)	Silva et al. (2010)
	4904 $\text{mg g}^{-1}$	6		As(V)	Luther et al. (2012)
Fh/amorphous	513 $\mu\text{mol g}^{-1}$	7	0.01	As(III)	Pierce and Moore (1982)
	1.258 $\text{mmol g}^{-1}$ ; 0.0047 $\text{mmol m}^{-2}$	5.0	0.01	As(V)	Silva et al. (2010)

Fe Oxide	3514 $\mu\text{mol g}^{-1}$	8	0.01	As(III)	Dixit and Hering (2003)
	909.09 - 169.67 $\mu\text{mol g}^{-1}$	8-10.5	0.01	As(V)	Hsia et al. (1992)
	2675 $\mu\text{mol g}^{-1}$	4	0.01	As(V)	Dixit and Hering (2003)
Al hydroxide	1600 – 501 $\mu\text{mol g}^{-1}$	5-9		As(V)	Anderson et al. (1976)
Gibbsite	$1.5 \cdot 10^{-8}$ - $2.6 \cdot 10^{-8}$ $\text{mol m}^{-2}$	4-8.2	0.01	As(III)	Weerasooriya et al. (2003)
	3.3 $\text{mg g}^{-1}$	5.5	0.15	As(III)	Ladeira et al. (2004) <sup>§</sup>
	0.0025-0.0054-0.0058 $\text{mmol m}^{-2}$	5-7-9	0.1	As(III)	Duarte et al. (2012)
	300-151 $\text{mmol kg}^{-1}$	4-7	0.05	As(V)	Violante and Pigna (2002)
	4.6 $\text{mg/g}$ ( $4.54 \mu\text{mol m}^{-2}$ )	5.5	0.15	As(V)	Ladeira et al. (2004)
	0.228 $\text{mmol g}^{-1}$ ; 0.0050 $\text{mmol m}^{-2}$	5.0	0.01	As(V)	Silva et al. (2010)
Kaolinite	10.0-8.1 $\text{mmol kg}^{-1}$	4-7	0.05	As(V)	Violante and Pigna (2002)
	< 0.23 $\text{mg g}^{-1}$	5.5		As(V)	Ladeira et al. (2004)
Calcite	<< 0.05 $\mu\text{mol m}^{-2}$	7.53	0.073	As(III)	So et al. (2008)
	$10^{-2.19}$ $\text{mol kg}^{-1}$	8.3		As(V)	Alexandratos et al. (2007)
	0.42 - 0.88 $\mu\text{mol m}^{-2}$	7.53 -8.03	0.073-0.004	As(V)	So et al. (2008)

<sup>†</sup>Maximum adsorption capacity; <sup>‡</sup>Ionic Strength (M); <sup>§</sup> Oxides from natural sources

Table 2: Specific surface area (SSA), point of zero charge (PZC),  $\zeta$  potential and particle equivalent hydrodynamic diameter ( $d_z$ ) of the adsorbing minerals

	SSA $\text{m}^2 \text{g}^{-1}$	PZC	$\zeta$ potential at pH 6.5 mV	$d_z$ at pH 6.5 $\mu\text{m}$
Ferrihydrite	317±10.4 <sup>†</sup>	8.2±0.26	22±0.8	1.2±0.02
KGa2-Fh	48±3.4	8.1±0.29	7±1.8	1.0±0.04
Hematite	46±2.8	6.3±0.39	-16±1.8	0.8±0.05
Goethite	44±1.6	8.0±0.17	20±0.9	1.3±0.05
Al-Goethite	40±2.0	7.3±0.26	4±1.0	1.0±0.03
Gibbsite	60±1.9	7.6±0.23	40±3.1	1.0±0.09
Al-hydroxide	498±11.8 <sup>‡</sup>	7.5±0.42	33±2.2	1.1±0.07
Kaolinite	21±0.7	4.8±0.14	-8±1.3	1.2±0.04
Calcite	2.8±0.12	nd	26±3.0	1.1±0.01

<sup>†</sup> Mean ± standard deviation

<sup>‡</sup> Determined by adsorption of H<sub>2</sub>O

Table 3: Langmuir parameters for As(III) and As(V) adsorption.  $X_{MAX}$  is the Langmuir maximum adsorption capacity;  $K_L$  is the Langmuir affinity constant

	As (III)				As (V)				As(III)/As(V)	
	$X_{MAX}$		$K_L$	$r^2$	$X_{MAX}$		$K_L$	$r^2$	$X_{MAX}$	$K_L$
	$\mu\text{mol g}^{-1}$	$\mu\text{mol m}^{-2}$	$\text{L mol}^{-1} (\times 10^{-4})$		$\mu\text{mol g}^{-1}$	$\mu\text{mol m}^{-2}$	$\text{L mol}^{-1} (\times 10^{-4})$			
Ferrihydrite	$1676 \pm 14^\dagger$	$5.28 \pm 0.15$	$23 \pm 2.2$	0.991	$904 \pm 30$	$2.85 \pm 0.12$	$29 \pm 0.8$	0.999	1.85	0.77
KGa2-Fh	$162 \pm 7.8$	$3.36 \pm 0.26$	$20 \pm 1.8$	0.989	$103 \pm 6.7$	$2.14 \pm 0.17$	$36 \pm 0.8$	0.998	1.57	0.56
Hematite	$71 \pm 0.4$	$1.55 \pm 0.09$	$5.4 \pm 0.33$	0.991	$39 \pm 1.4$	$0.85 \pm 0.05$	$15 \pm 3.9$	0.999	1.84	0.35
Goethite	$99 \pm 0.4$	$2.25 \pm 0.07$	$43 \pm 2.2$	0.999	$75 \pm 1.6$	$1.71 \pm 0.06$	$64 \pm 0.6$	0.998	1.32	0.67
Al-Goethite	$41 \pm 1.8$	$1.03 \pm 0.06$	$20 \pm 3.4$	0.998	$32 \pm 1.3$	$0.79 \pm 0.04$	$92 \pm 10$	0.999	1.30	0.22
Al-hydroxide	$566 \pm 31$	$1.13 \pm 0.06$	$0.3 \pm 0.04$	0.855	$1350 \pm 34$	$2.71 \pm 0.08$	$11 \pm 0.8$	0.998	0.42	0.02
Gibbsite	$0.6 \pm 0.03$	$0.01 \pm 0.0004$	$4.9 \pm 0.48$	0.975	$54 \pm 2.5$	$0.88 \pm 0.04$	$8.0 \pm 3.1$	0.997	0.01	0.61
Kaolinite	$1.4 \pm 0.02$	$0.07 \pm 0.002$	$5.3 \pm 0.19$	0.799	$4.5 \pm 0.21$	$0.21 \pm 0.01$	$18 \pm 6.3$	0.982	0.31	0.30
Calcite	$0.1 \pm 0.004$	$0.04 \pm 0.002$	$10 \pm 1.2$	0.899	$0.8 \pm 0.11$	$0.28 \pm 0.03$	$13 \pm 2.6$	0.996	0.16	0.77

<sup>†</sup> Mean  $\pm$  standard deviation

Table 4. Heat of adsorption ( $\Delta H$ ) values of arsenite and arsenate adsorption on amorphous Al-hydroxide, gibbsite, goethite, ferrihydrite (Fh), and kaolinite-ferrihydrite (KGa2-Fh) systems determined by isothermal titration calorimetric measurements.

	$\Delta H$ (kJ mol <sup>-1</sup> )	
	As(III)	As(V)
Goethite	- 26.4 ± 1.6	- 44.1 ± 1.3
Fh <sup>†</sup>	- 32.9 ± 2.0	- 45.1 ± 1.8
KGa2-Fh <sup>†</sup>	- 24.4 ± 2.7	- 39.9 ± 3.3
Al hydroxide	+ 7.1 ± 4.4	- 28.8 ± 4.5
Gibbsite	+ 0.68 ± 2.0	- 21.6 ± 1.1

<sup>†</sup> Data from Martin et al. (2009)

Table 5: Adsorbent concentration ( $\text{g L}^{-1}$ ) necessary to reach an equilibrium concentration in solution ( $C_e$ ) of 0.05 or 0.01  $\text{mg L}^{-1}$  of As(III) or As(V) at pH 6.5 from an As initial concentration of 1  $\text{mg L}^{-1}$ .

	As(III)		As(V)	
	( $C_e = 0.05 \text{ mg L}^{-1}$ )	( $C_e = 0.01 \text{ mg L}^{-1}$ )	( $C_e = 0.05 \text{ mg L}^{-1}$ )	( $C_e = 0.01 \text{ mg L}^{-1}$ )
Ferrihydrite	$9.7 \times 10^{-2}$	$4.7 \times 10^{-1}$	$8.6 \times 10^{-2}$	$3.9 \times 10^{-1}$
KGa2-Fh	$7.5 \times 10^{-1}$	$3.6 \times 10^0$	$7.1 \times 10^{-1}$	$3.2 \times 10^0$
Hematite	$5.1 \times 10^0$	$2.6 \times 10^1$	$3.5 \times 10^0$	$1.7 \times 10^1$
Goethite	$6.3 \times 10^{-1}$	$2.8 \times 10^0$	$1.3 \times 10^0$	$5.8 \times 10^0$
Al-Goethite	$2.7 \times 10^0$	$1.3 \times 10^1$	$1.6 \times 10^0$	$6.8 \times 10^0$
Gibbsite	$6.6 \times 10^2$	$3.4 \times 10^3$	$4.6 \times 10^0$	$2.3 \times 10^1$
Al-hydroxide	$1.2 \times 10^1$	$6.5 \times 10^1$	$1.3 \times 10^{-1}$	$6.6 \times 10^{-1}$
Kaolinite	$2.5 \times 10^2$	$1.3 \times 10^3$	$2.7 \times 10^1$	$1.3 \times 10^2$
Calcite	$1.2 \times 10^3$	$5.9 \times 10^3$	$2.0 \times 10^2$	$9.8 \times 10^2$

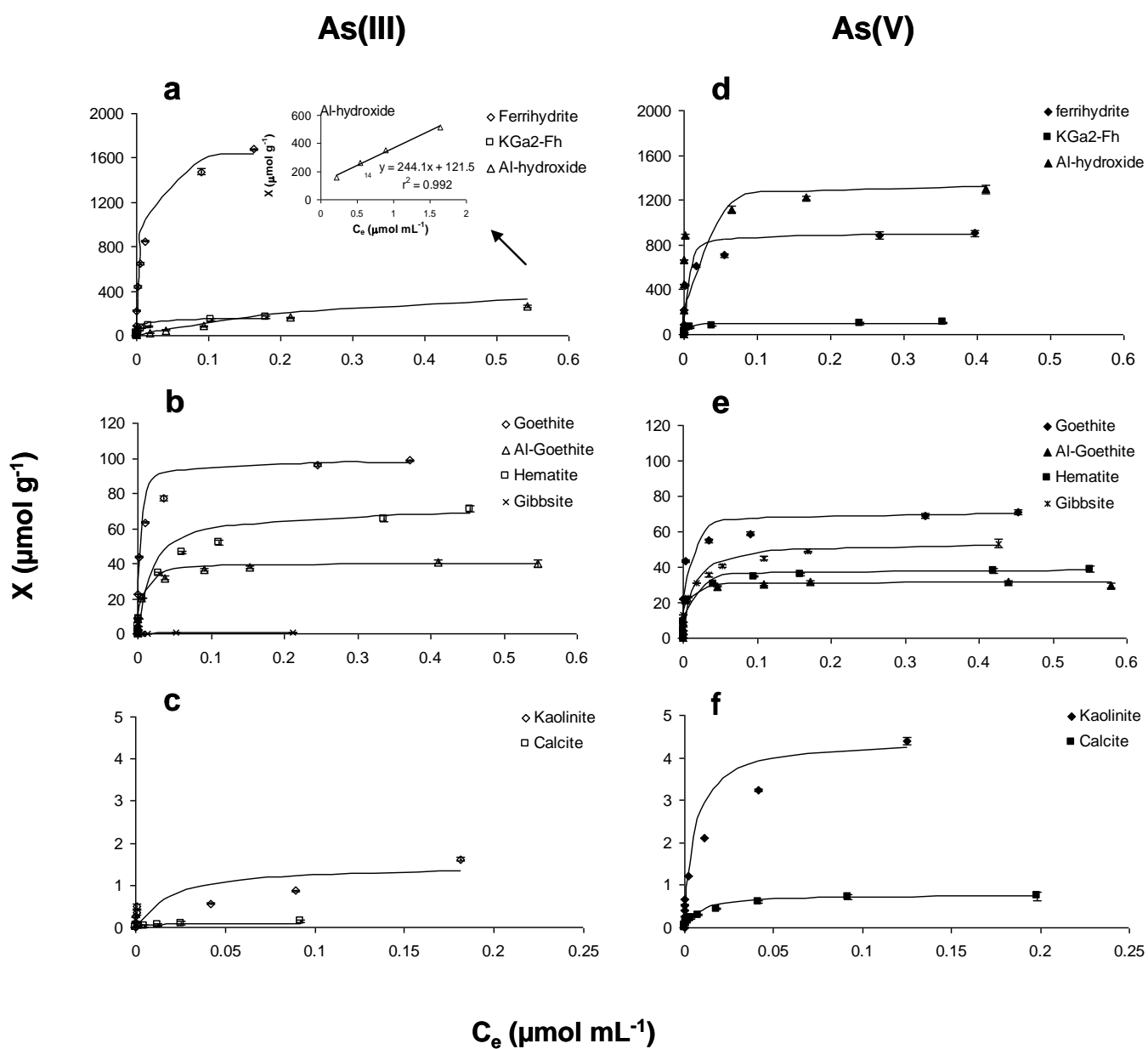


Figure 1. Arsenite and arsenate adsorption isotherms on: poorly crystalline Fe and Al oxides and KGa2-Fh (a, d); crystalline Fe oxides and gibbsite (b, e); kaolinite and calcite (c,f). Error bars represent standard deviation

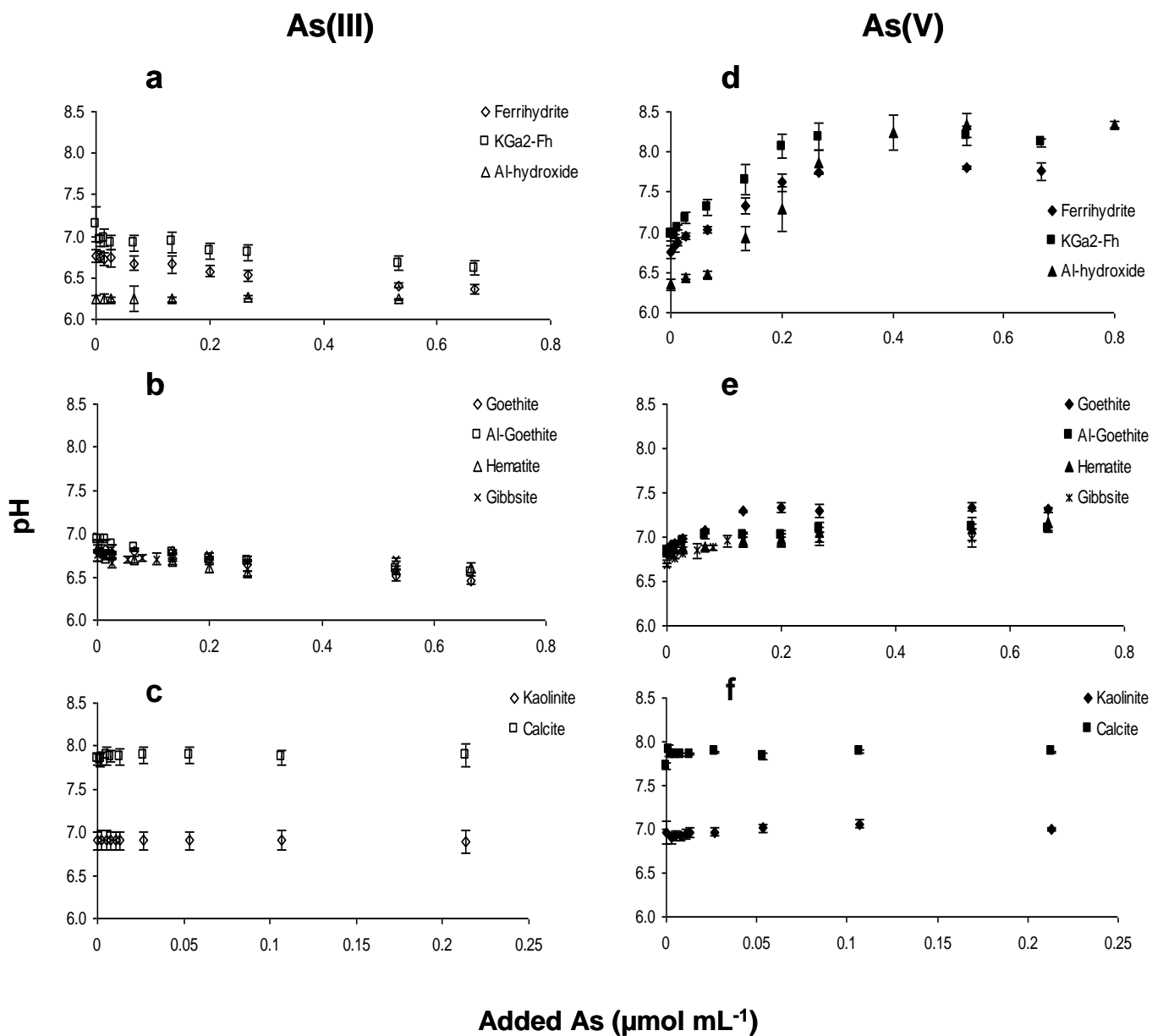


Figure 2. Effect of arsenite and arsenate adsorption on the pH of: poorly crystalline Fe and Al oxides and KGa2-Fh (a, d); crystalline Fe oxides and gibbsite (b, e); kaolinite and calcite (c, f). Error bars represent standard deviation

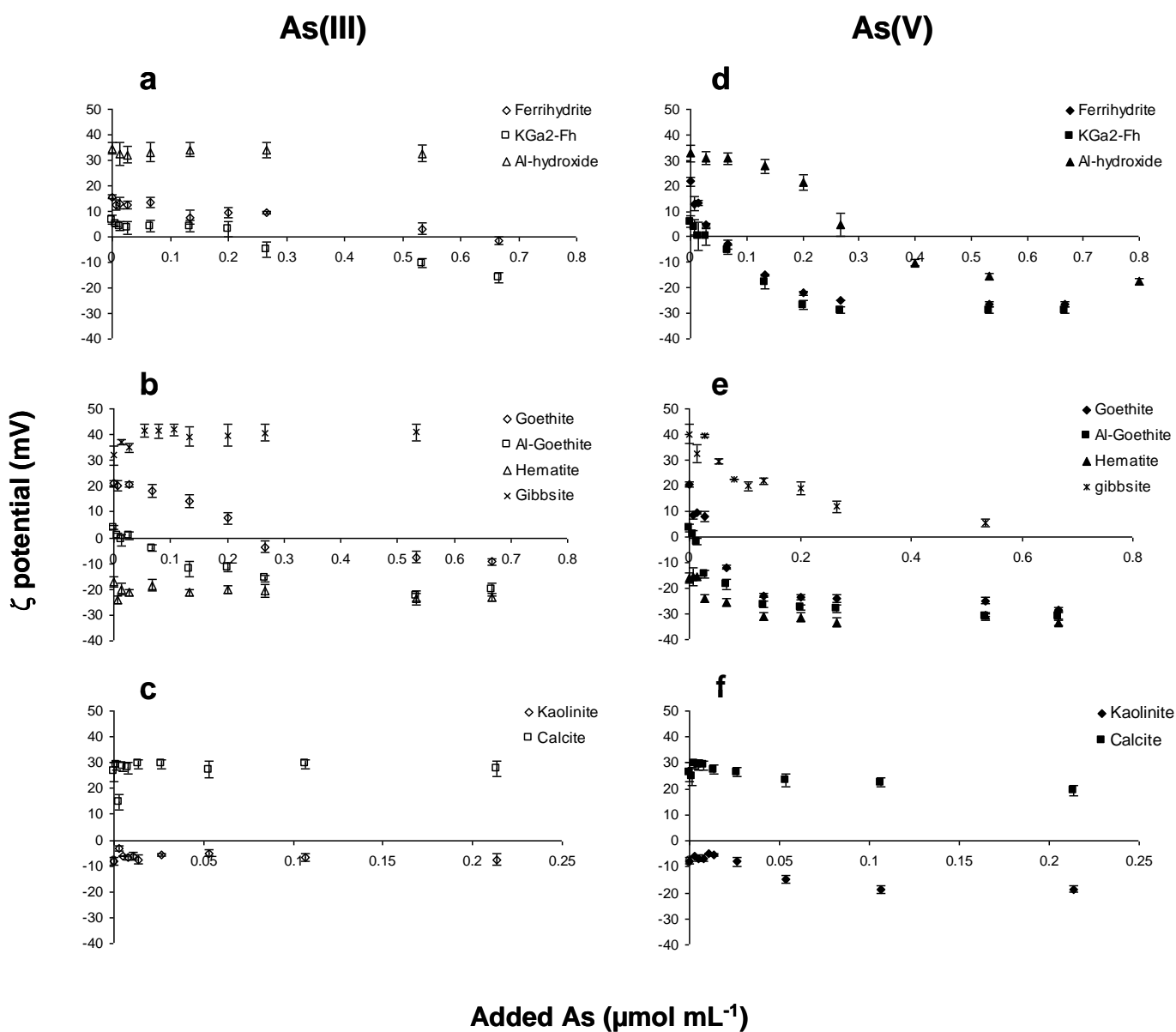


Figure 3. Effect of arsenite and arsenate adsorption on the  $\zeta$  potential of: poorly crystalline Fe and Al oxides and KGa2-Fh (a, d); crystalline Fe oxides and gibbsite (b, e); kaolinite and calcite (c, f). Error bars represent standard deviation

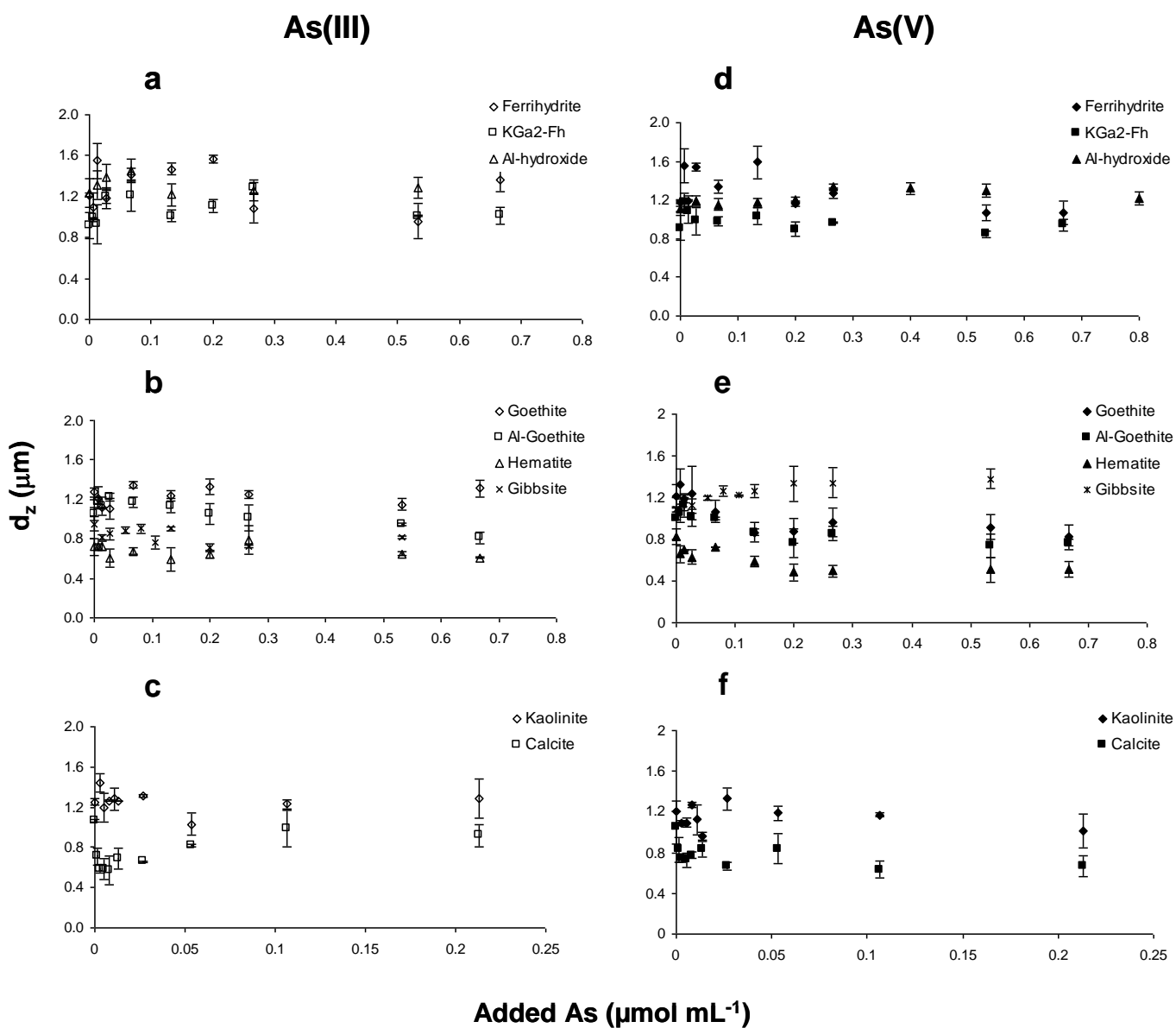


Figure 4. Effect of arsenite or arsenate adsorption on the particle equivalent hydrodynamic diameter ( $d_z$ ) of: poorly crystalline Fe and Al oxides and KGa2-Fh (a, d); crystalline Fe oxides and gibbsite (b, e); kaolinite and calcite (c, f). Error bars represent standard deviation